PHYSICAL REVIEW B **85**, 060201(R) (2012)

Short-range structural signature of excess specific heat and fragility of metallic-glass-forming supercooled liquids

Jun Ding,[1] Yong-Qiang Cheng,[1] Hongwei Sheng,[2] and Evan Ma[1,*]

[1]*Department of Materials Science and Engineering, Johns Hopkins University, Baltimore, Maryland 21218, USA*

[2]*School of Physics, Astronomy and Computational Sciences, George Mason University, Fairfax, Virginia 22030, USA*

(Received 13 January 2012; published 13 February 2012)

Supercooled metallic liquids exhibit very different temperature (T) dependence of the excess specific heat (ΔC_p) and viscosity, profoundly influencing their glass-forming ability. Using two model glass-forming liquids in molecular dynamics simulation, here we demonstrate that their contrasting ΔC_p and relaxation/viscosity behavior has an underlying origin in their different T-dependent local structural ordering. Upon undercooling toward glass transition, a particularly stabilizing type of short-range ordering that accelerates with decreasing T leads to a steeply rising ΔC_p and higher fragility, whereas local motifs that merely respond to the densification of the liquids result in a weak T dependence of ΔC_p.

DOI: 10.1103/PhysRevB.85.060201 PACS number(s): 64.70.pe, 61.20.Ja

The specific heat (C_p) is a fundamental property of materials, and especially important for those supercooled liquids, from which bulk metallic glasses (BMGs) form via cooling of the melts.[1] In particular, how C_p evolves with temperature (T) during undercooling strongly correlates with the fragility of the liquid[2] and the glass-forming ability (GFA)[3] of the molten alloy. C_p versus T behavior of two glass-forming liquids, Cu-Zr [4] and Pd-Ni-Cu-P,[5] is shown in Fig. 1. For these two examples, C_p was measured experimentally over a wide range of temperatures in the supercooled liquid. This was possible for the Pd-Ni-Cu-P liquid because of its extraordinary resistance to crystallization (high GFA),[5] and for the marginal BMG former Cu-Zr[6] thanks to the use of an electrostatic levitation technique that allowed large undercooling.[4] We observe in Fig. 1 contrasting C_p behavior in terms of the T dependence: Pd-Ni-Cu-P exhibits a shallow C_p curve (weakly T sensitive), whereas that of Cu-Zr shows a very obvious rising trend.

The contrasting C_p behaviors suggest that the intrinsic material state (i.e., inherent structure) must evolve with supercooling in different ways and at different rates. This structural origin is expected, because a different T dependence of the configurational entropy of the liquid, $S_c(T)$, is the root cause of the different C_p behavior, as $(\frac{\partial S_c}{\partial T})_p = \frac{\Delta C_p}{T}$, where ΔC_p is the "excess specific heat," i.e., the difference in constant-pressure specific heat between the quasi-equilibrium supercooled liquid and the frozen glass.[7] To rephrase this, $\Delta C_p(T)$ is determined by the reduction rate of $S_c(T)$ as the liquid is cooled, such that the underlying structural basis for the different T dependence of C_p should lie in how fast the atoms order themselves to reduce $S_c(T)$. How different this structural evolution would look, in terms of short-range ordering (SRO), and how this can lead to the different C_p behavior known for many supercooled liquids that have been experimentally characterized,[3] remains largely unknown for realistic alloy liquids and is therefore of general interest (although model Lennard-Jones systems have been studied before[8–10]). This Rapid Communication illustrates this fundamental structural origin by providing a detailed, microscopic picture of the different structural evolution that can be responsible, respectively, for the flat versus fast-ascending C_p curves. This connection is extended then to correlate with and explain the different dynamical properties (relaxation time and viscosity) of two binary alloy liquids.

To access atomistic details, we use molecular dynamics (MD) simulations of two different MG-forming model binary alloy supercooled liquids. Model I uses embedded atom method (EAM) interatomic potentials for Cu-Zr, at the composition of $Cu_{64}Zr_{36}$,[11] representing a system that undergoes considerable icosadedral SRO in the liquid.[12] Model II is based on EAM potentials fitted to the Pd-Si system (see Ref. 13 for details of the method/data (Refs. 14–19) empolyed for potential development) that features solute-solute avoidance and solute-centered trigonal prisms as the local SRO in the liquid (for example for some metal-metalloid systems near the 80-20 composition, specifically $Pd_{82}Si_{18}$). While these computer liquid models are expected to have similar local structural motifs when compared with real-world liquids (those in Fig. 1), they are subject to very different spatiotemporal and sample preparation conditions. As such, they are only meant to show that they can also exhibit the different heat capacity and fragility trends known for real alloys, but a perfect match with the experimentally measured property values would not be expected. For each model, a series of 10,000-atom liquid configurations from 2000 to 300 K (at the interval of 20 K) was obtained via *NPT* quenching (at zero pressure) from the equilibrium melt (2000 K) at the rate of 10^{10} K/s. At each temperature in the supercooled regime, the configuration was relaxed for 10–100 ns until the total energy leveled off. The relaxed configurations were run under *NPT* at zero pressure for another 10 ns to produce 200 samples at each temperature, from which an average is obtained for the properties to be evaluated. Voronoi tessellation was used to analyze the inherent structure.[25,26] The enthalpy (H) was calculated for zero pressure, including both kinetic and potential energies.

The two model supercooled liquids feature contrasting behavior in C_p. Figure 2(a) displays the enthalpy (H) calculated for $Cu_{64}Zr_{36}$ between 900 and 1220 K. C_p, which is shown in Fig. 2(b), is obtained from the fluctuation of enthalpy in liquids, according to $\langle \delta(U+PV)^2 \rangle_{NPT} = k_B T^2 C_p$, where $\langle \delta(U+PV)^2 \rangle = \langle (U+PV)^2 \rangle - \langle (U+PV) \rangle^2$, and U is the sum of potential and kinetic energy.[20] The H-T relation in Fig. 2(a) exhibits a clear deviation from linearity, and was

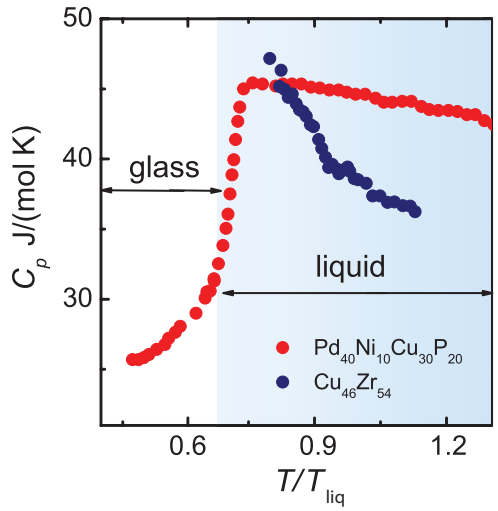

FIG. 1. (Color online) Experimental data of specific heat in the liquid/glassy state for two metallic-glass-forming systems. Cu-Zr data are taken from Ref. 4 and Pd-Ni-Cu-P data are taken from Ref. 5.

fit using an equation $H = a\ \ln(T) + bT^2 + cT + d$, where a, b, c, d are fitting parameters. This equation was chosen because it is consistent with the Vogel-Fulcher-Tammann (VFT)[21] description of viscosity $\eta = A\ \exp[\frac{B}{T-T_0}]$,[23] and the Adam-Gibbs theory[7] $\eta = A\ \exp[\frac{B}{TS_c(T)}]$, where A, B, and T_0 are fitting parameters (more discussions are presented in Ref. 13). C_p can then be alternatively determined by taking the first derivative of this H-T curve; this approach yielded consistent results with those in Fig. 2(b). One observes a pronounced C_p rise, showing a trend very similar to the experimental data measured for a similar binary $Cu_{46}Zr_{54}$ MG-forming supercooled liquid[4] (see Fig. 1, and many other MG-forming liquids[3,24]). We also calculated the enthalpy data of the solid $Cu_{64}Zr_{36}$ MG configurations between 500 and 600 K and derived their C_p. ΔC_p at $T_g$can be estimated (following Ref. 27) to be about 14 J/(mol K), in reasonable agreement with known experimental data for a number of BMGs.[27]

The behavior of the $Pd_{82}Si_{18}$ model supercooled liquid is also shown in Fig. 2. The H-T relation is quite different from

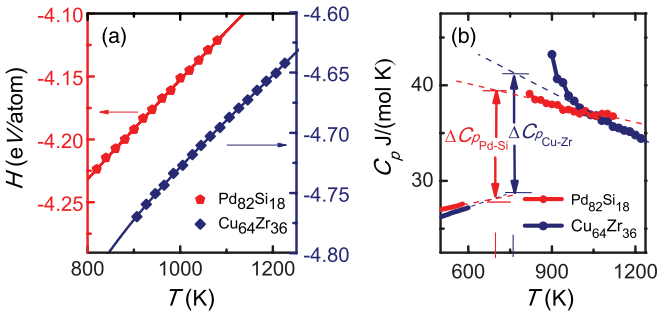

FIG. 2. (Color online) (a) Calculated enthalpy (symbols) of the supercooled liquids for $Cu_{64}Zr_{36}$ and $Pd_{82}Si_{18}$ in computer simulation. The lines are the fitted H-T curves.[13] (b) Specific heat (C_p) calculated using the fluctuation method (also see in Ref. 13 similar results from the derivative method) for Cu-Zr and Pd-Si (the respective ΔC_p at T_g is also marked).

that of $Cu_{64}Zr_{36}$ discussed above, with much less curvature, as shown in Fig. 2(a). The $C_p(T)$ curve in Fig. 2(b) calculated using the fluctuation method (and the derivative approach as well) is rather flat, much less T-dependent than the Cu-Zr case. This resembles some MG-forming liquids, such as the one in Fig. 1. Having obtained the contrasting ΔC_p behavior in our two model liquids, the next step is to analyze the structural origin responsible, which may shed light on the different ΔC_p behavior in real-world MG-forming supercooled liquids.

Before analyzing the role of structural evolution during cooling in controlling C_p, we note that for $Cu_{64}Zr_{36}$ at all temperatures the enthalpy of all the Cu atoms is an almost fixed fraction, 0.480 ± 0.002, of the total system H. Taking them to be representative of the whole system, in the following we will therefore examine the energies of Cu atoms and will focus on all the Cu-centered coordination polyhedra, to uncover the structural evolution responsible for the H change. A similar scaling is also found for $Pd_{82}Si_{18}$: the contribution of the minority (solute Si) atoms to the system H is also a constant fraction of 0.2086 ± 0.0004 at all temperatures.

We now monitor the structural features throughout the supercooled liquid regime. For $Cu_{64}Zr_{36}$, the five most frequent Voronoi indices are ⟨0 0 12 0⟩, ⟨0 2 8 2⟩, ⟨0 2 8 1⟩, ⟨0 2 8 0⟩, ⟨0 3 6 3⟩, for the Cu-centered polyhedral; see their evolution in Fig. 3(a). To find out how each one contributes to the bending of the H-T in Fig. 2(a), we separate and plot in Fig. 3 their individual contributions. Because the total kinetic energy of the

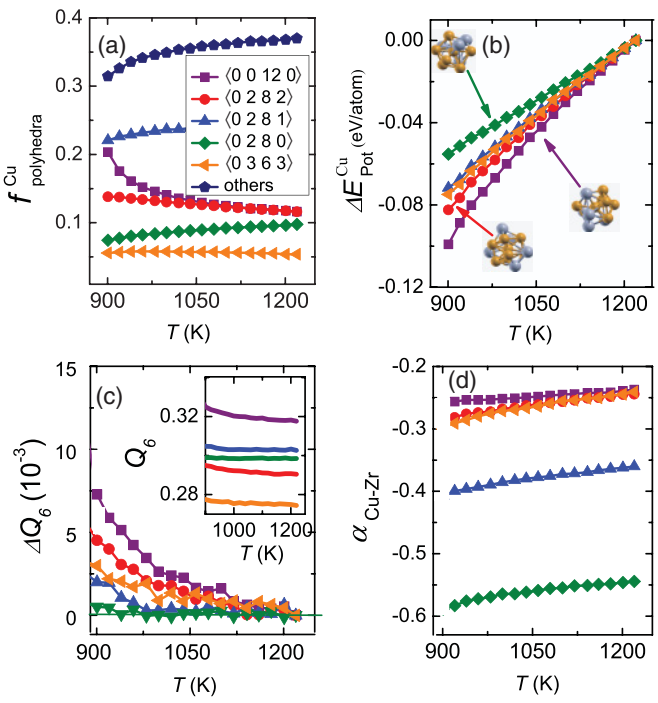

FIG. 3. (Color online) SRO analysis of $Cu_{64}Zr_{36}$ supercooled liquid. (a) Fractions of the most frequent Cu-centered polyhedra. (b) Potential energy difference of Cu atoms in several key polyhedra, relative to the reference state at 1220 K. Insets show three representatives: ⟨0 0 12 0⟩, ⟨0 2 8 2⟩, and ⟨0 2 8 0⟩. (c) ΔQ_6 (change of Q_6 with reference state at 1220 K). Inset shows the Q_6 evolution for each type of polyhedra. (d) CSRO.

Cu atoms in the centers of the polyhedra shows a linear relation with T, contributing only a constant value to C_p, we can just focus on the potential energy ($E_{\rm pot}$) change of Cu centers and relate their contribution to their structural ordering. Figure 3(b) plots the change of $E_{\rm pot}$, on a per atom basis and relative to the value at 1220 K, for Cu center atoms in polyhedra of different indices. It is obvious that the average $E_{\rm pot}$ of Cu centers inside full icosahedra (FI), with Voronoi index ⟨0 0 12 0⟩, have dropped nonlinearly with decreasing T much faster than all the others. A similar trend is observed, but to a lower degree, for the other polyhedra with a coordination number (CN) of 12, such as ⟨0 2 8 2⟩, which can be viewed as more distorted icosahedra. In comparison, Cu centers in ⟨0 2 8 0⟩ polyhedra displayed a nearly linear relation. Moreover, we see in Fig. 3(a) that the fraction of Cu-centered FI (⟨0 0 12 0⟩), which has lower $E_{\rm pot}$ relative to others [Fig. 3(b)], rises significantly upon cooling toward T_g at the expense of other polyhedra (the fraction of FI reaches ∼0.21, much greater than a previous simulation at the same temperature,[12] because of the prolonged MD relaxation to reach a quasiequilibrium supercooled liquid state in this study). The above results suggest that the excess specific heat, i.e., the fast rise of ΔC_p with decreasing T in the supercooled liquid region, is due to the extraordinary enthalpy reduction associated with icosahedral ordering.

The nonlinear reduction of average $E_{\rm pot}$ with decreasing T for Cu atoms embedded in FI can be attributed to the improved icosahedral symmetry, as revealed by the bond orientational order parameter (BOP).[28] Specifically, the BOP of neighboring atoms surrounding the center atom can be quantified using a set of spherical harmonics, so that different types of local order often yield different values. For example, $\overline{Q_6}$, which is an effective indicator of icosahedral order,[28] increases at lower temperatures, particularly strongly in FI [inset in Fig. 3(c)]. This improvement in symmetry renders the atoms more comfortable, lowering their energy and configurational entropy. In contrast with this trend of improved topological order in icosahedra and distorted icosahedra [see the relative change of BOP in Fig. 3(c)], the ⟨0 2 8 0⟩ polyhedra exhibit almost constant $\overline{Q_6}$across the entire T range. The dramatic increase of FI fraction, which is another aspect of the growing icosahedral order as discussed in the last paragraph, compounding the symmetry improvement of the average FI to reduce the enthalpy, constitutes the topological signature underlying the fast-ascending ΔC_p.

As for chemical short-range order (CSRO), the Warren-Cowley parameter (α_{AB}) was used to characterize the chemical makeup of the nearest-neighbor pairs.[29] Figure 3(d) demonstrates a more negative CSRO in the polyhedra with undercooling, indicating the increasing preference for more unlike (Cu-Zr) bonds that reduce energy. Note that the CSRO is not independent of topological order and goes hand in hand with icosahedral ordering,[11] facilitating the latter. The simulation results above are consistent with the experimental trend found by Wessels *et al.* [4]

We next demonstrate that, in the absence of such structural ordering through the supercooled liquid region, C_p stays rather flat as opposed to fast rising. We illustrate this using the model II liquid, $Pd_{82}Si_{18}$. For the four most frequent polyhedra in this alloy [Fig. 4(a)], which are also known to dominate for metal-metalloid amorphous alloys,[26,30] ⟨0 3 6 0⟩, ⟨0 4 4 0⟩, ⟨0 2 8 0⟩, ⟨0 3 6 1⟩, the $E_{\rm pot}$ decreases with T are all approximately linear with very close slopes, as seen in Fig. 4(b), contributing a constant to C_p. The fractions of these local motifs apparently all follow a linear T dependence, reminiscent of the H-T behavior in Fig. 2(a). With cooling, the atomic packing density increases and the denser polyhedra (CN = 9 in this case) become more preferable at the expense of looser ones (e.g., CN = 8). However, there is no accelerated increase in a particular SRO that preferentially lowers enthalpy as the icosahedra order does in the $Cu_{64}Zr_{36}$ case. Also, there is no improvement in symmetry of the clusters [see the constant BOP in Fig. 4(c)], nor additional CSRO [Fig. 4(d)] because all of the solute Si center atoms are always surrounded by the solvent Pd as nearest neighbors.[26,30] The result is a rather flat C_p.

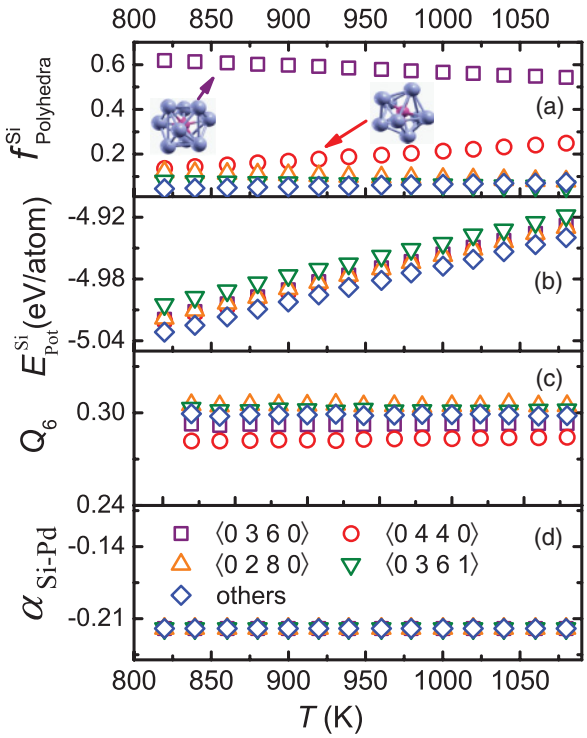

FIG. 4. (Color online) (a) Fractions, (b) potential energy, (c) Q_6, and (d) CSRO of the typical Si-centered polyhedra in $Pd_{82}Si_{18}$. Insets in (a) are two representative Si-centered polyhedra, ⟨0 3 6 0⟩ and ⟨0 4 4 0⟩.

As hinted by the Adam-Gibbs equation,[7,13] the structural evolution responsible for S_c and C_p is also expected to influence the T dependence of the dynamics (such as viscosity) of the liquid, but this is rarely demonstrated for realistic alloys.[8,31–33] Figure 5 compares the α-relaxation time (τ) for all species in both $Cu_{64}Zr_{36}$ and $Pd_{82}Si_{18}$ liquids (see Refs. 13 and 20–22 for methods). The solid lines are VFT[21] fittings for the Si and Zr data. In each liquid, the absolute τ value may vary with different species (dashed line versus solid line), but the trend is almost identical (see caption of Fig. 5 and Ref. 13). Figure 5 demonstrates that $Cu_{64}Zr_{36}$ liquid is more fragile than $Pd_{82}Si_{18}$. In the inset, we also present viscosity (η) data (calculated via the Green-Kubo equation[20]) and VFT fitting for the two liquids. Although it is difficult for computer simulation to assess viscosity at low temperatures,

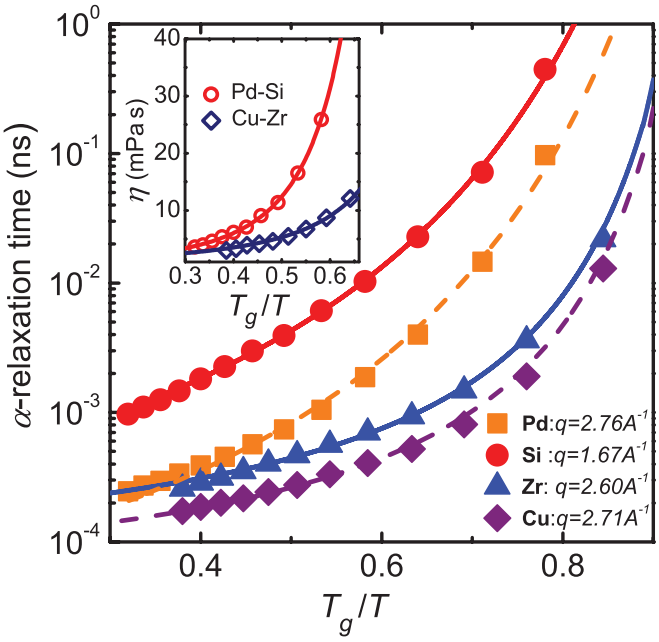

FIG. 5. (Color online) α-relaxation time (symbols) for each species in $Cu_{64}Zr_{36}$ and $Pd_{82}Si_{18}$ liquids. The data can be well represented by VFT fitting (solid lines for the minority species and dashed lines for majority species). See Ref. 13 for more information about the fitting and the wave vector q. Taking Cu as the representative of Cu-Zr (Zr shows very similar behavior) to compare with either Pd or Si (the two species share a similar trend), the Cu-Zr is apparently a more fragile liquid than Pd-Si. The same conclusion is also obvious from the inset, which shows viscosity data for $Cu_{64}Zr_{36}$ and $Pd_{82}Si_{18}$ liquids and their VFT fitting (solid lines).

the trend seen here is consistent with the assessment of fragility difference given by the τ data. The observed difference in the T dependence of τ or η is not surprising, as we have shown earlier that $Cu_{64}Zr_{36}$ undergoes more dramatic local structural ordering than $Pd_{82}Si_{18}$, and hence a steeper rise of configurational entropy, with T decreasing toward T_g. In other words, the ascending C_p-T curve and higher fragility, i.e., the two key thermodynamic and kinetic properties, correlate with one another[3] and have common origin in the atomic-level structural evolution.

In conclusion, we have demonstrated that an extraordinary rise in excess specific heat can arise from the increasing development of structural ordering, and in particular the icosahedra SRO in the model I ($Cu_{64}Zr_{36}$) supercooled liquid. The increasingly fast drop of H with undercooling comes especially from icosahedral clusters: the latter increase in their number population and improve in their local symmetry and CSRO. The resulting change in the curvature of the H-T curve is responsible for the fast rising C_p. As the rate of structural ordering accelerates when approaching T_g (Fig. 2 and Fig. 3), so does the reduction of configurational entropy and the rise in $\eta(T)$ or $\tau(T)$. In contrast, for model II ($Pd_{82}Si_{18}$), because all the order parameters (number of preferred lower-enthalpy polyhedra, topological SRO, and CSRO) scale almost linearly with the decreasing T, so does the enthalpy and its derivative ΔC_p is thus not too far from being constant during undercooling. This implies a much weaker T dependence of $S_c(T)$ and a more fragile behavior compared with the model I liquid. We note that one needs to exercise caution when interpreting the properties of a specific liquid in experiment, as there may be other factors beyond the SRO types discussed in our models that influence the experimentally observed varying behaviors (e.g., Fig. 1 and Ref. 3). However, it is clear from our study that, in general, structural ordering plays a key role in controlling the heat capacity behavior of supercooled liquids. The local structure evolution is also a signature indicator of the dynamical behavior. An expected correlation is that escalating ordering with undercooling underlies the ascending heat capacity, leading at the same time to a more pronounced deviation from the Arrhenius behavior (linear in Angell plot) and higher fragility.

This work was supported by the US National Science Foundation, Division of Materials Research, under Contracts No. NSF-DMR-0904188 and No. NSF-DMR-0907325.

*ema@jhu.edu

[1] A. L. Greer and E. Ma, MRS Bull. **32**, 611 (2007).
[2] C. A. Angell, MRS Bull. **33**, 5 (2008).
[3] R. Busch, J. Schroers, and W. H. Wang, MRS Bull. **32**, 620 (2007).
[4] V. Wessels, A. K. Gangopadhyay, K. K. Sahu, R. W. Hyers, S. M. Canepari, J. R. Rogers, M. J. Kramer, A. I. Goldman, D. Robinson, J. W. Lee, J. R. Morris, and K. F. Kelton, Phys. Rev. B **83**, 094116 (2011).
[5] I.-R. Lu, G. Wlide, G. P. Gorler, and R. Willnecker, J. Non-Cryst. Solids **250-252**, 577 (1999).
[6] D. Wang, Y. Li, B. B. Sun, M. L. Sui, K. Lu, and E. Ma, Appl. Phys. Lett. **84**, 4029 (2004).
[7] G. Adam and J. H. Gibbs, J. Chem. Phys. **43**, 19 (1965).
[8] D. Coslovich and G. Pastore, J. Chem. Phys. **127**, 124504 (2007).
[9] H. G. E. Hentschel, V. Ilyin, and I. Procaccia, Phys. Rev. Lett. **101**, 265701 (2008).
[10] U. R. Pedersen, T. B. Schroder, J. C. Dyre, and P. Harrowell, Phys. Rev. Lett. **104**, 105701 (2010).
[11] Y. Q. Cheng, H. W. Sheng, and E. Ma, Phys. Rev. Lett. **102**, 245501 (2009) [the potential file is available on the website. http://sites.google.com/a/gmu.edu/eam-potential-database/].
[12] Y. Q. Cheng, H. W. Sheng, and E. Ma, Phys. Rev. B **78**, 014207 (2008).
[13] See Supplemental Material at http://link.aps.org/supplemental/10.1103/PhysRevB.85.060201, which also contains Refs. 14–24.
[14] VASP, G. Kresse and J. Furthmüller, Comput. Mater. Sci. **6**, 15 (1996).
[15] P. E. Blöchl, Phys. Rev. B **50**, 17953 (1994).
[16] G. Kresse and D. Joubert, Phys. Rev. B **59**, 1758 (1999).
[17] P. Brommer and F. Gähler, Modelling Simul. Mater. Sci. Eng. **15**, 295 (2007).

[18]H. W. Sheng, M. J. Kramer, A. Cadien, T. Fujita, and M. W. Chen, Phys. Rev. B **83**, 134118 (2011).

[19]P. Villars and L. D. Calvert, *Pearson's Handbook of Crystallographic Data for Intermetallic Phases*, 2nd ed. (ASM International, Materials Park, Ohio, 1991).

[20]M. P. Allen and D. J. Tildesley, *Computer Simulation of Liquids* (Clarendon Press, Oxford, 1987).

[21]H. Vogel, Z. Phys. **22**, 645 (1921); G. S. Fulcher, Am. Ceram. Soc. Bull. **8**, 339 (1925); G. Tammann and G. Hesse, Z. Anorg. Allg. Chem. **156**, 245 (1926).

[22]W. Kob and H. C. Andersen, Phys. Rev. E **52**, 4134 (1995).

[23]C. A. Angell, Science **267**, 1924 (1995).

[24]Y. Zhang, N. Mattern, and J. Eckert, J. Appl. Phys. **110**, 093506 (2011).

[25]G. Voronoi and J. Reine, Angew. Math. **134**, 198 (1908).

[26]H. W. Sheng, W. K. Luo, F. M. Alamgir, J. M. Bai, and E. Ma, Nature (London) **439**, 419 (2006).

[27]H. B. Ke, P. Wen, D. Q. Zhao, and W. H. Wang, Appl. Phys. Lett. **96**, 251902 (2010).

[28]P. J. Steinhardt, D. R. Nelson, and M. Ronchetti, Phys. Rev. B **28**, 784 (1983).

[29]B. E. Warren, *X-ray Diffraction* (Dover Publications, New York, 1990); J. M. Cowley, J. Appl. Phys. **21**, 24 (1950).

[30]Y. Q. Cheng and E. Ma, Prog. Mater. Sci. **56**, 379 (2011).

[31]H. Shintani and H. Tanaka, Nature Phys. **2**, 200 (2006).

[32]M. Dzugutov, S. I. Simdyankin, and F. H. M. Zetterling, Phys. Rev. Lett. **89**, 195701 (2002).

[33]I. Ladadwa and H. Teichler, Phys. Rev. E **73**, 031501 (2006).